

**[Supporting information] of**

**Defective acidic 2D COF based catalysts for boosting performance of polyoxymethylene diethyl ethers synthesis under mild conditions**

Guoqin Wang,<sup>[a,b]</sup> Gangli Zhu,<sup>\*[a,b,d]</sup> Yong Ding,<sup>[c]</sup> Chungu Xia,<sup>[a,d]</sup> Fang Wang,<sup>[a]</sup> and Zhen Li<sup>\*[a]</sup>

<sup>[a]</sup>State Key Laboratory for Oxo Synthesis and Selective Oxidation, Suzhou Research Institute of *LICP*, Lanzhou Institute of Chemical Physics (*LICP*), Chinese Academy of Sciences, Lanzhou 730000, China

<sup>[b]</sup>University of Chinese Academy of Sciences, Beijing 100049, China

<sup>[c]</sup>College of chemistry and chemical engineering, Lanzhou University, Lanzhou 730000, China

<sup>[d]</sup>Dalian National Laboratory for Clean Energy, Chinese Academy of Sciences, Dalian 116023, China

\*Corresponding authors' E-mail: zhugl@licp.cas.cn; zhenli@licp.cas.cn;

## Contents

|            |   |             |
|------------|---|-------------|
| Section 1  | Experimental details                              | Pages 1-3   |
| Section 2  | N <sub>2</sub> sorption characterizations of MPCP | Pages 4-6   |
| Section 3  | TG/DSC analysis                                   | Page 7      |
| Section 4  | PXRD analysis                                     | Page 8      |
| Section 5  | FT-IR analysis                                    | Pages 9-10  |
| Section 6  | Indicator titration method                        | Pages 11-12 |
| Section 7  | UV-Vis analysis                                   | Pages 13-14 |
| Section 8  | XPS analysis                                      | Pages 15-20 |
| Section 9  | Effect of reaction temperature                    | Page 21     |
| Section 10 | Effect of reaction time                           | Page 22     |
| Section 11 | Effect of catalyst content                        | Page 23     |
| Section 12 | Simulated structure of MPCP                       | Page 24     |
| Section 13 | Simulated structure of PCP                        | Page 25     |
| Section 14 | DFT calculation of reactants                      | Pages 26-28 |

## **Section 1. Experimental details**

### **1.1 Chemicals and materials**

Diethoxymethane (DEM, 99.5%) was purchased from Energy Chemical and trioxane (TOX, 99.5%) was provided by Aladdin. Before the reaction, DEM was dehydrated with calcined 4A Na-type zeolite, and TOX was recrystallized with dehydrated cyclohexane. Phthalic anhydride, pyromellitic dianhydride, anhydrous cobalt chloride,  $(\text{NH}_4)_2\text{Mo}_2\text{O}_7$  were obtained from Adamas. Urea and  $\text{NH}_4\text{Cl}$  were provided by Greagent. Reagents including acetone, methanol, tetrahydrofuran (THF), concentrated sulphuric acid (98%), ethyl acetate, sodium sulphite, *p*-toluenesulfonic acid and phosphoric acid mentioned in this work were of analytical grade and used without further purification. Deionized water was produced by Millipore water purifier.

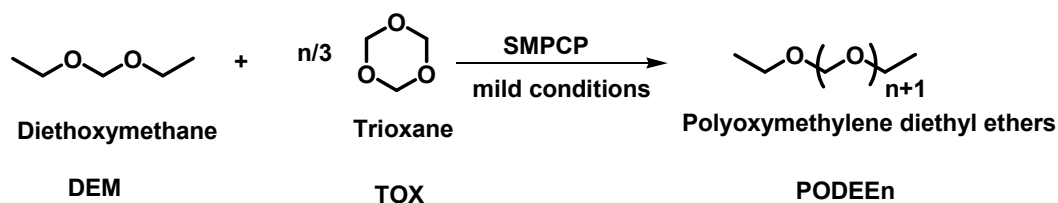
### **1.2 Catalyst preparation**

The phthalocyanine containing polymers material (PCP) can be synthesized by a facile and effective method<sup>[1,2]</sup>. Firstly, 1.44g pyromellitic dianhydride, 0.39g anhydrous cobalt chloride, 2.46g urea, 0.6g  $\text{NH}_4\text{Cl}$  and 0.015g  $(\text{NH}_4)_2\text{Mo}_2\text{O}_7$  were ground and calcined at 220 °C for 3h to obtain the dark green powers. After washing with deionized water, acetone and methanol for three times, the powders were dried at 80 °C in a vacuum drying oven for 12 h. Then PCP precursor via self-polymerization was sulfonated by excessive concentrated sulfuric acid to gain the sulfonated phthalocyanine containing polymers catalyst (SPCP).

To introduce more network defects, the mixing polymerization of phthalic anhydride and pyromellitic dianhydride method was used. Typically, 0.72g phthalic anhydride, 0.72g pyromellitic dianhydride, 0.39g anhydrous cobalt chloride, 2.46g urea, 0.6g  $\text{NH}_4\text{Cl}$  and 0.015g  $(\text{NH}_4)_2\text{Mo}_2\text{O}_7$  were mixed together and ground into powders in a mortar. Then the powders were transformed into a 100 mL ceramic crucible and calcined in a muffle furnace at 220 °C for 3h in air. The resulting solids were cooled down to room temperature, washed with deionized water, acetone and methanol for three times. Afterwards, the solids were dried at 80 °C in a vacuum drying oven for 12 h. Then, the MPCP precursor gained by mixing polymerization was sulfonated at 180 °C for 12 h with excessive concentrated sulfuric acid. After cooling down to room temperature, the sulfonated powders were precipitated with ethyl acetate. Then, and the solids were washed with ethyl acetate for 5 times and dried in vacuum at 80 °C for 12 h to gain the acidic sulfonated phthalocyanine containing polymers by mixing polymerization (SMPCP).

### 1.3 The catalytic performance evaluation

The catalytic activity of SMPCP for the synthesis of polyoxymethylene diethyl ethers (PODEE<sub>n</sub>) was evaluated in mild reaction conditions. (**Scheme S1**).



**Scheme S1.** The synthesis process of PODEE<sub>n</sub> from DEM and TOX.

Typically, DEM (0.53 g), TOX (0.27 g) and catalyst of SMPCP (0.04 g) were

added into a flask and the reaction was carried out at 80 °C (atmospheric pressure) for 6 h with magnetic stirring. After the reaction, products mixture can be quantified by GC (Agilent 7890A), which was outfitted with a flame ionization detector (FID) and chromatographic column (AT-SE-54, 60m×0.25mm×0.25 mm).

The products were quantitatively analyzed using tetrahydrofuran (THF) as the internal standard compound according to the previous literature<sup>[3]</sup>. Formaldehyde (FA) can be determined by the sodium sulphite titration method<sup>[4]</sup>. The TOX conversion ( $C_{TOX}$ ) and the selectivity of  $PODEE_n$  ( $S_{PODEE_n}$ ) can be quantitatively calculated with following formulas.

$$C_{TOX} = \frac{m_{TOX,feed} - m_{TOX,product}}{m_{TOX,feed}} \times 100\% \quad (1)$$

$$S_i = \frac{m_{i,product}}{\sum m_{i,product}} \times 100\% \quad (2)$$

And the  $m_i$  is referring to the mass of product species  $i$  and  $\sum m_i$  is referring to the mass of all the liquid products after reaction.

## Section 2. N<sub>2</sub> sorption characterizations of MPCP

The N<sub>2</sub> sorption characterizations of MPCP and pore size distribution data were shown in Figure S1-3.

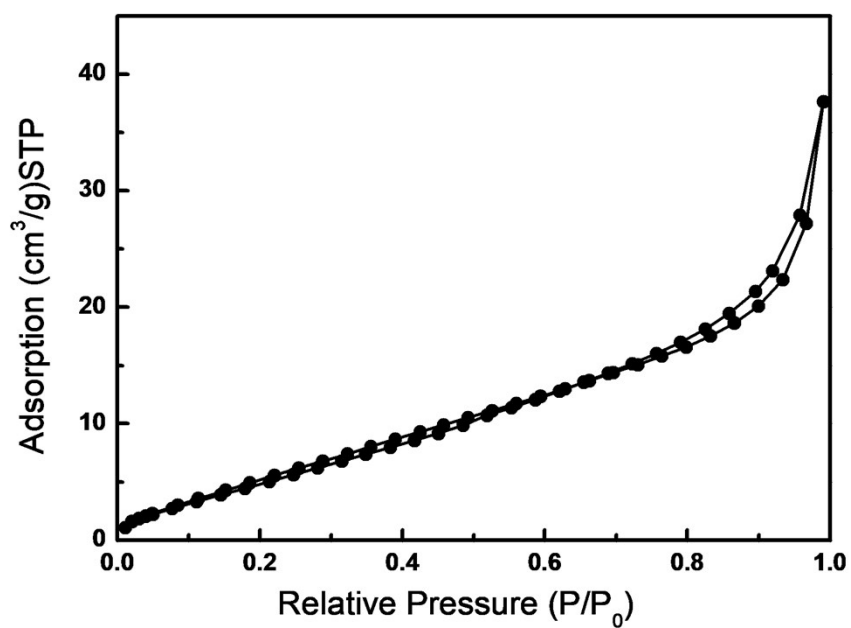


**Figure S1.** Nitrogen adsorption-desorption isotherms of MPCP.

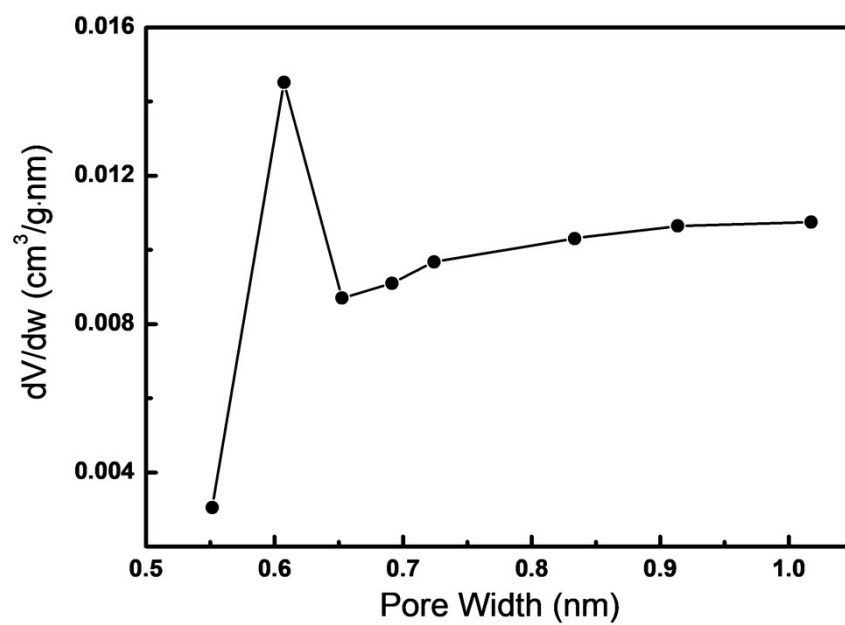


**Figure S2.** Microporous pore size distribution of MPCP.

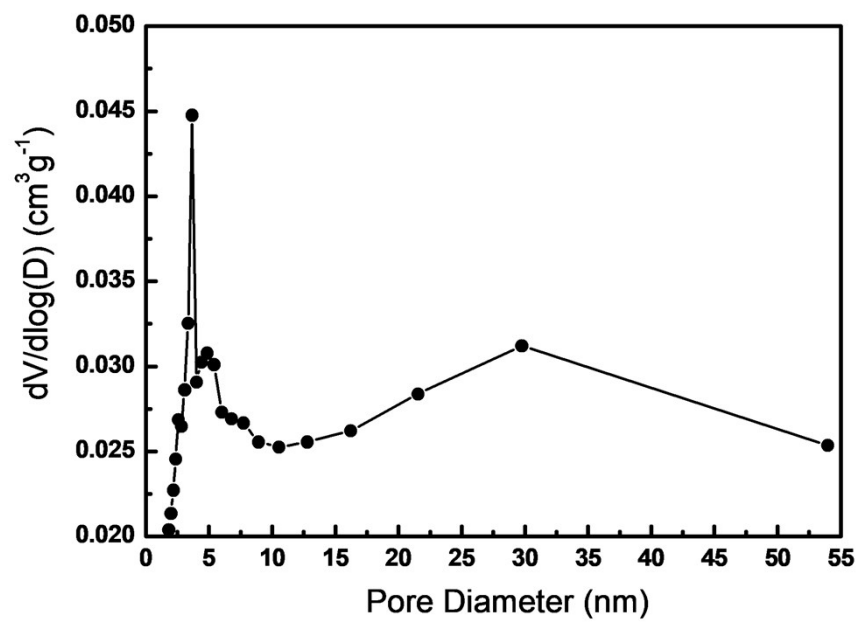


**Figure S3.** Mesoporous pore size distribution of MPCP.



### Section 3. TG/DSC analysis

TG/DSC curves of catalyst SMPCP were shown in Figure S4.

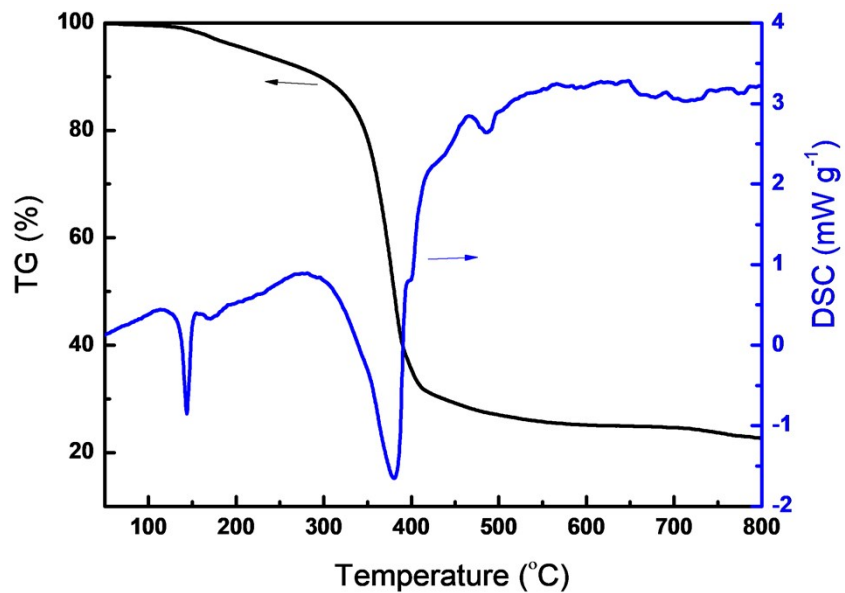


**Figure S4.** TG/DSC curves of catalyst SMPCP.

## Section 4. PXRD analysis

PXRD analysis of different samples CoPc and PCP were shown in Figure S5.

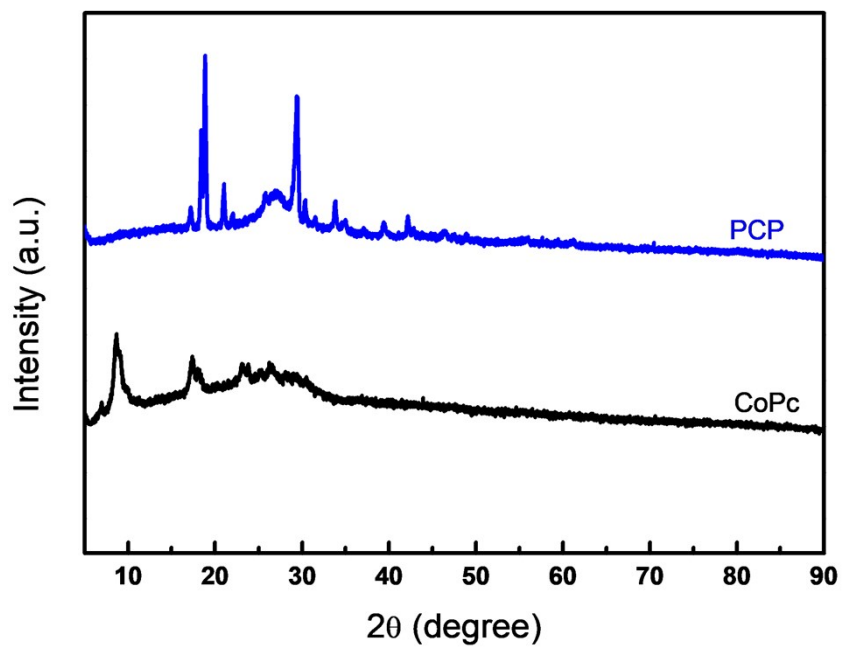


**Figure S5.** PXRD patterns of different samples. (a) PCP, (b) CoPc.

## Section 5. FT-IR analysis

FT-IR analysis of CoP<sub>C</sub>, PCP, MPCP, SPCP and SMPCP were conducted. And the results were shown in Figure S6 and Figure S7.

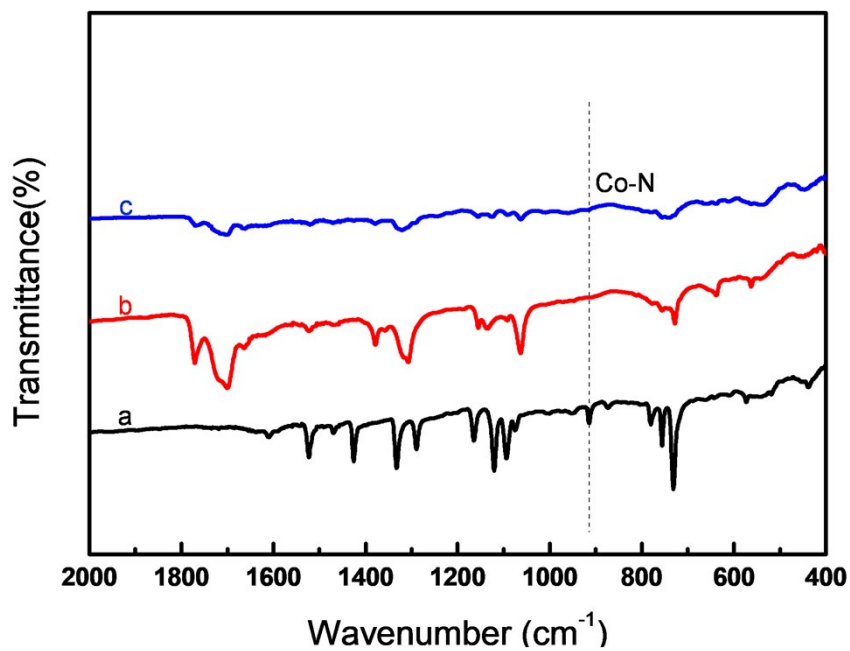


**Figure S6.** FT-IR spectra of (a) CoP<sub>C</sub>, (b) PCP, (c) MPCP.

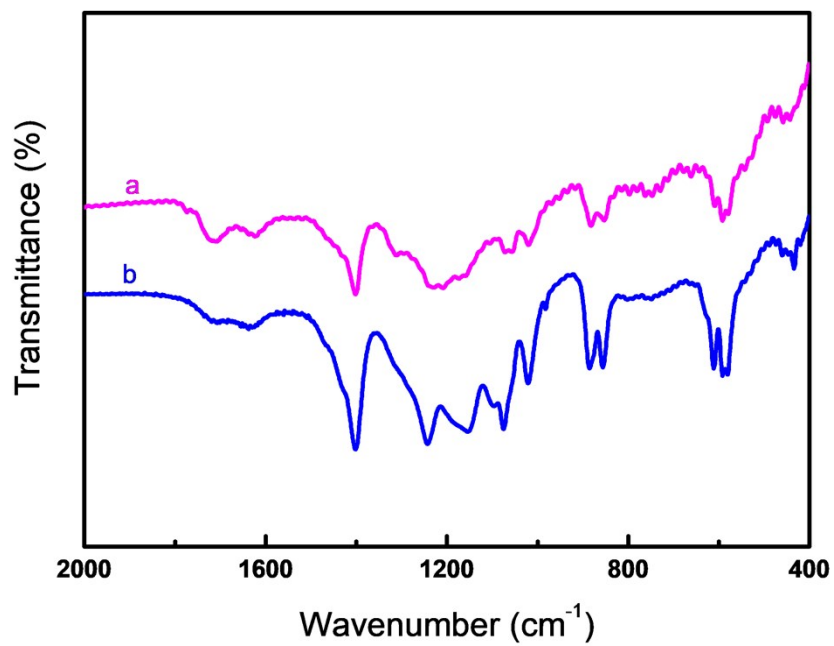


**Figure S7.** FT-IR spectra of different samples. (a) SPCP, (b) SMPCP.

## Section 6. Indicator titration method

The Hammett acidity was examined and acid-base titration of catalyst SMPCP was performed. The indicator discoloration was shown in Figure S8 and Figure S9.

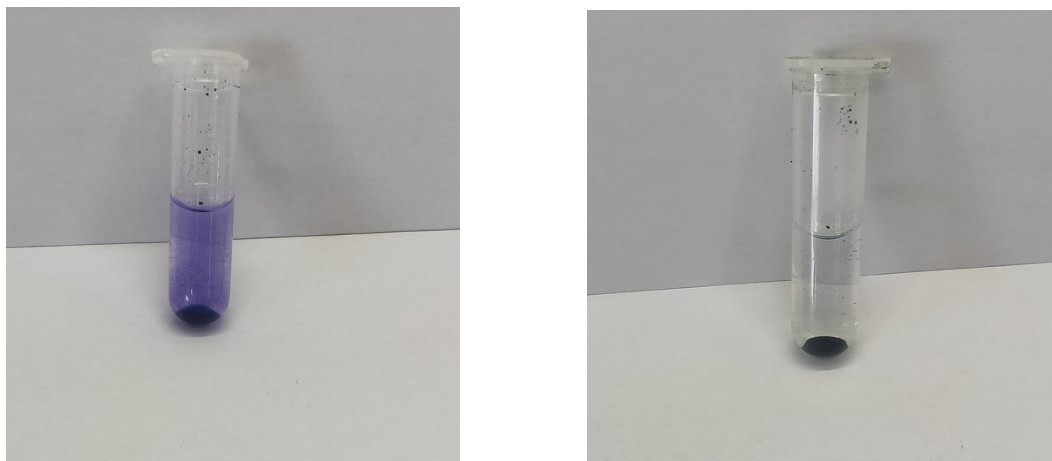


**Figure S8.** Gentian violet discoloration from purple to greenish yellow.  
(in the Hammett acidity examination)



(a)



(b)

**Figure S9.** Acid-base titration using methyl red as the indicator. The picture of indicator color: (a) before titration, and (b) after titration.

## Section 7. UV-Vis analysis

The UV-Vis spectra of MPCP and PCP were shown in Figure S10, and spectra of SMPCP and catalyst SMCPC after reaction were shown in Figure S11.

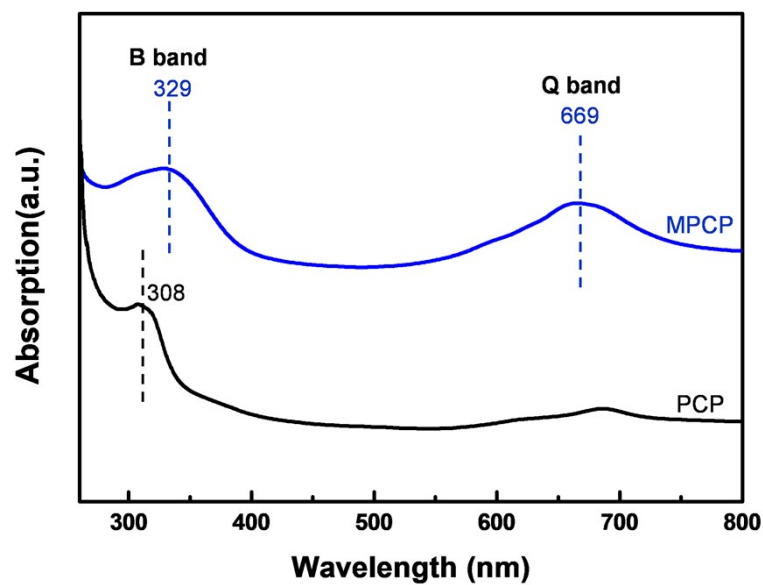


**Figure S10.** UV-Vis spectra of MPCP and PCP in DMSO solution.

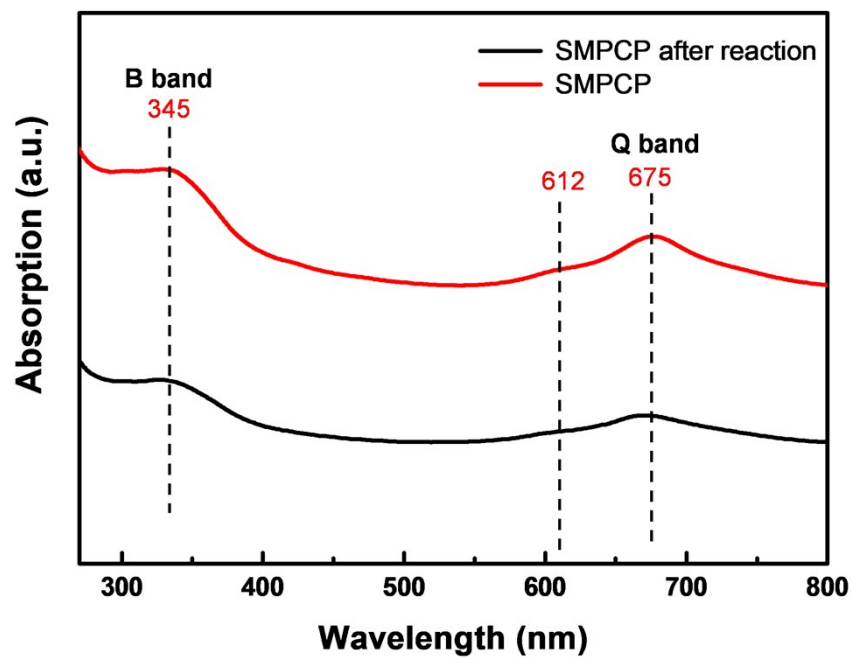


**Figure S11.** UV-*Vis* spectra of SMPCP and catalyst SMPCP after reaction in DMSO solution.



## Section 8. XPS analysis

XPS analysis of different samples was carried out, according to XPS semi-quantitative analysis, the content of cobalt in MPCP was 1.4%. The XPS spectra of MPCP, SMPCP and SMPCP after reaction were shown in Figure S12-S17.

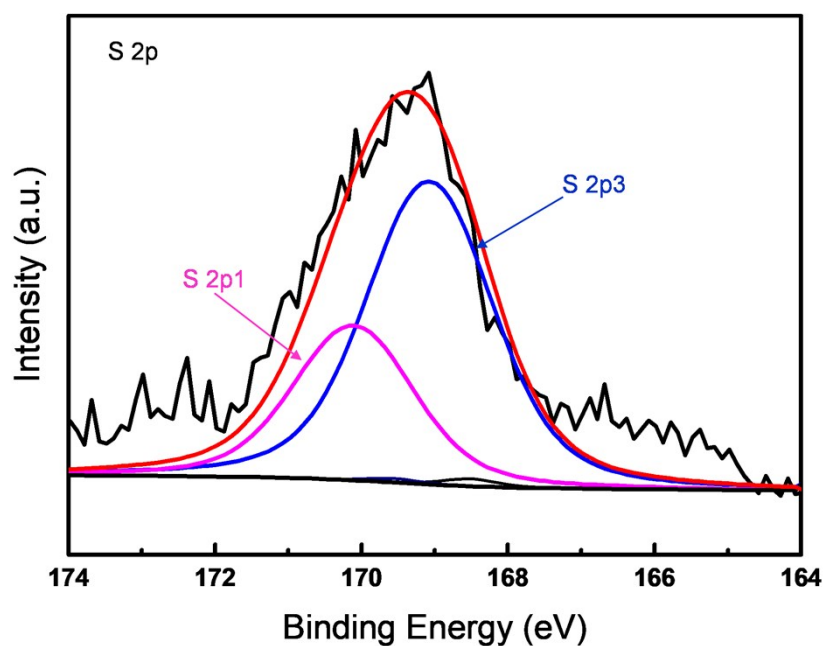


**Figure S12.** S 2p XPS spectrum of SMPCP.

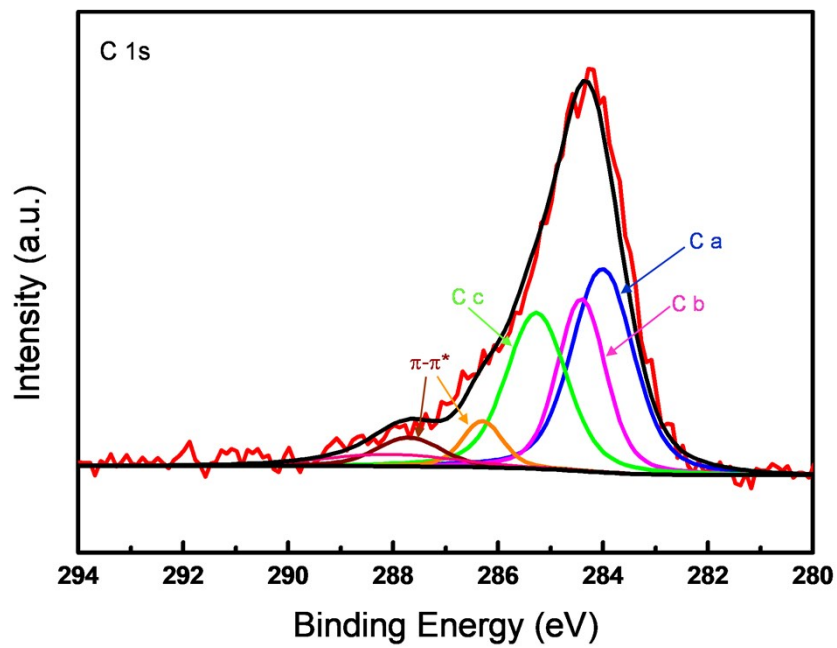


**Figure S13.** C 1s XPS spectrum of SMPCP.

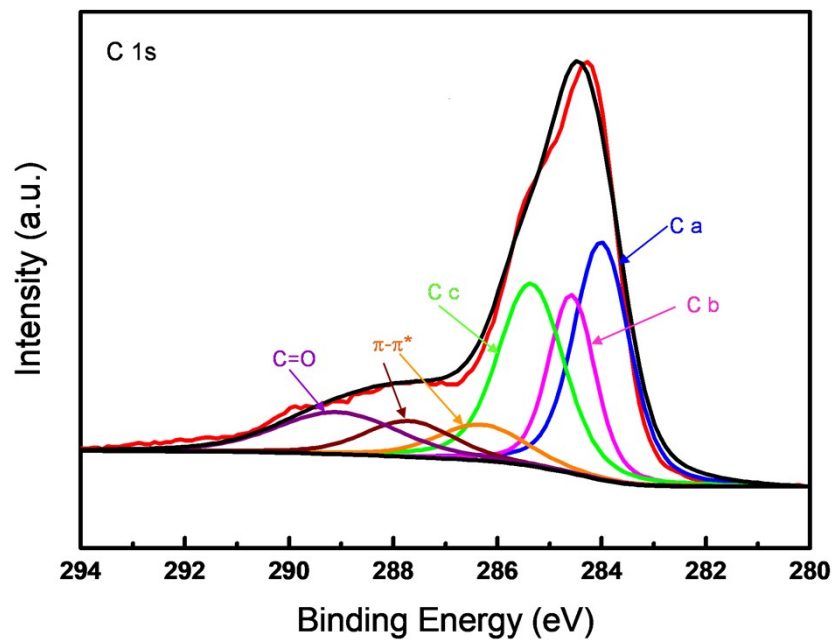


**Figure S14.** C 1s XPS spectrum of MPCP.

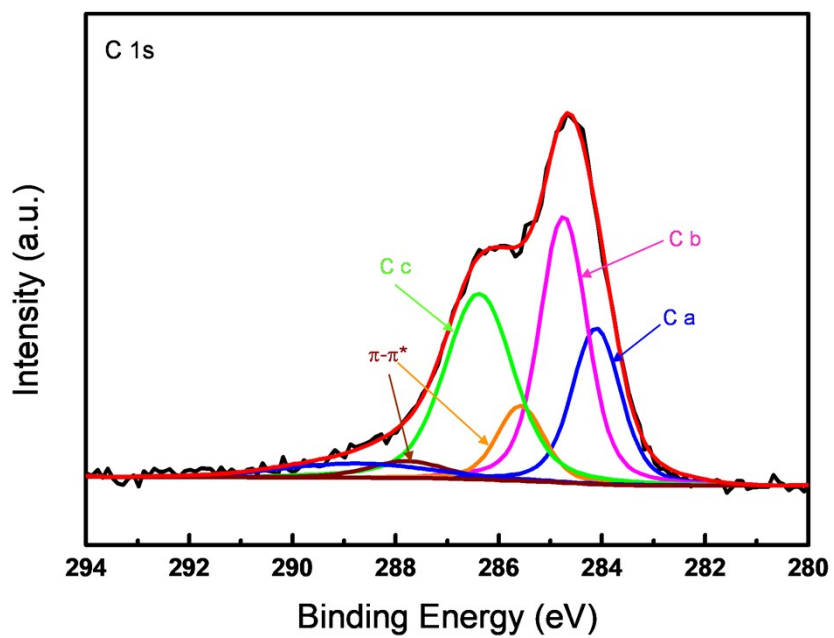


**Figure S15.** C 1s XPS spectrum of SMPCP after reaction.

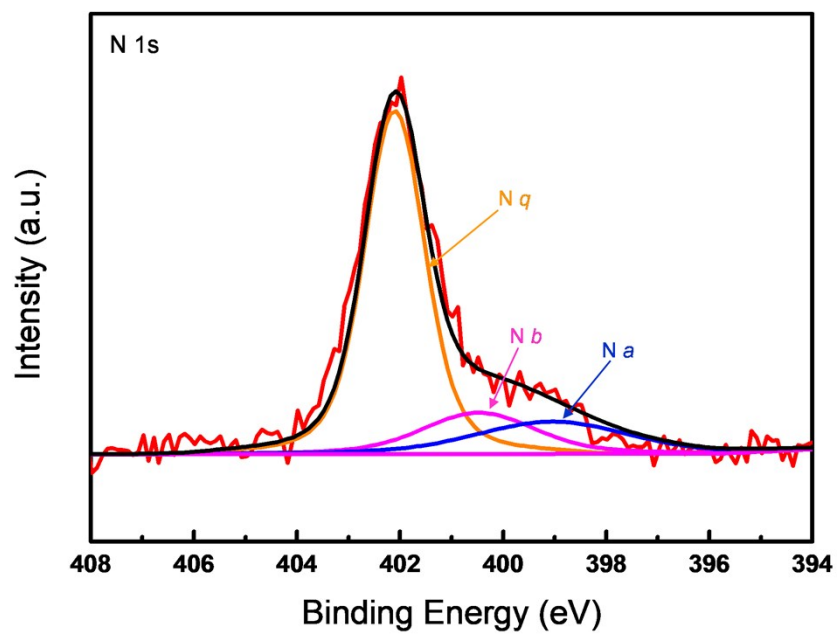


**Figure S16.** N 1s XPS spectrum of SMPCP after reaction.

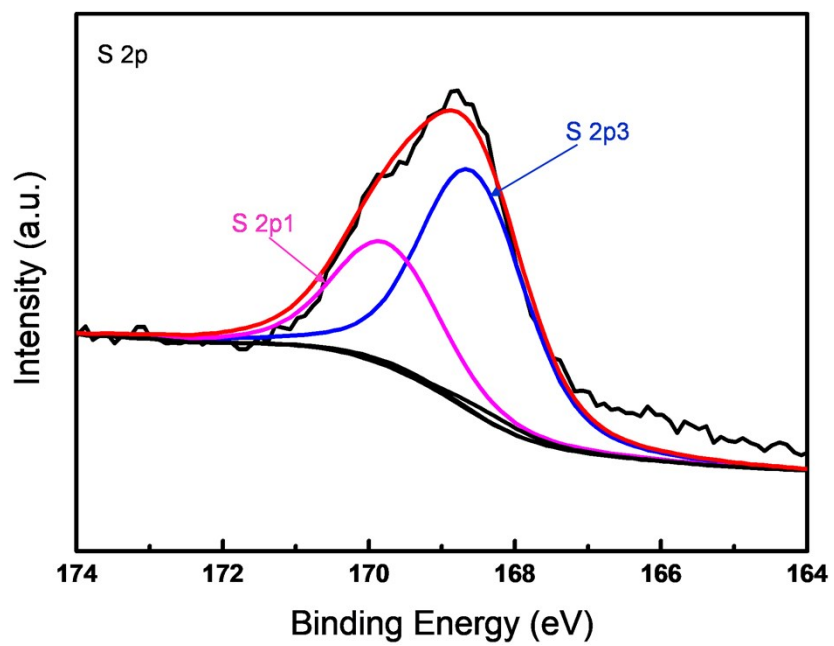


**Figure S17.** S 2p XPS spectrum of SMPCP after reaction.

## Section 9. Effect of reaction temperature

Effect of reaction temperature was examined and the results were shown in Figure S18.

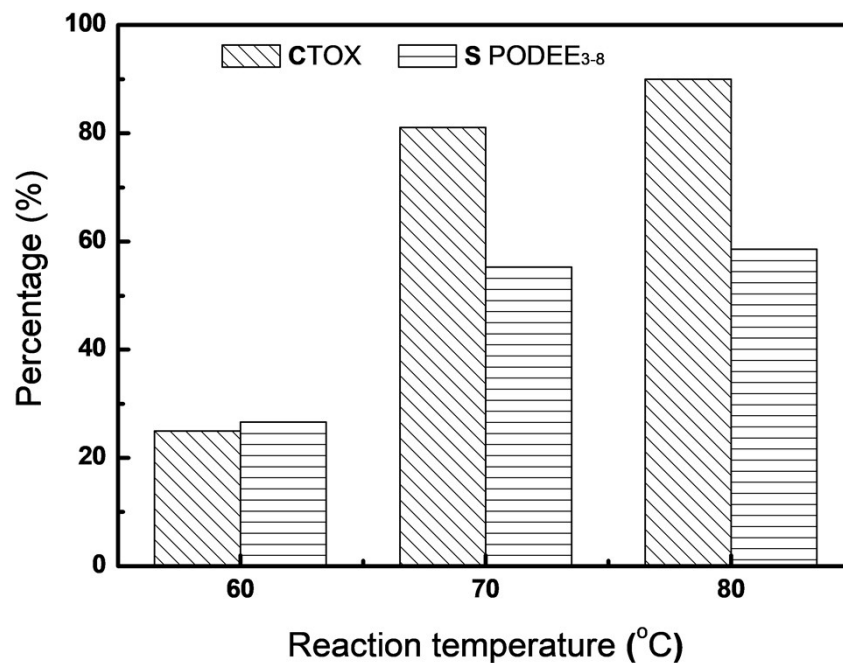


**Figure S18.** Effect of reaction temperature. Reaction conditions: 1 atm, 6h, m(DEM):m(TOX) mass ratio =2:1, m(catalyst) % = 5 wt%, catalyst: SMPCP.

## Section 10. Effect of reaction time

Effect of reaction time was examined and the results were shown in Figure S19.

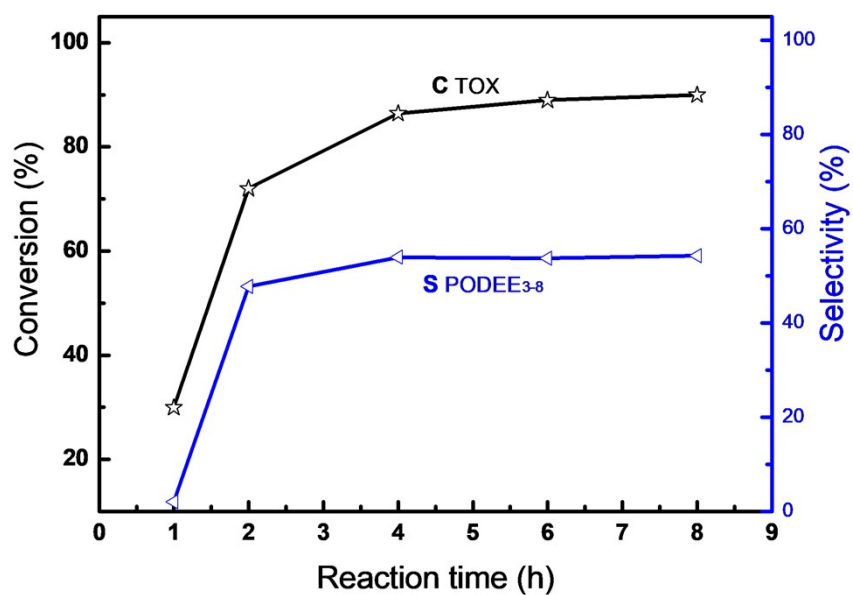


**Figure S19.** Effect of reaction time. Reaction conditions: 80 °C, 1 atm, m(catalyst)% =5wt%, m(DEM):m(TOX) mass ratio =2:1, catalyst: SMPCP.



## Section 11. Effect of catalyst content

Effect of catalyst content was investigated as shown in Figure S20.

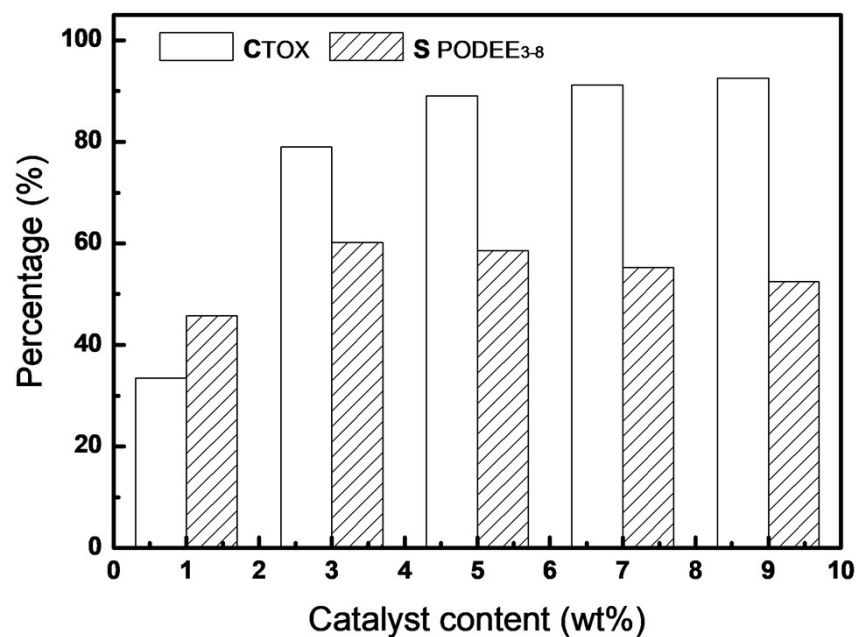


**Figure S20.** Effect of catalyst content. Reaction conditions: 80 °C, 1 atm, 6h, m(DEM):m(TOX) mass ratio =2:1, catalyst: SMPCP.

## Section 12. Simulated structure of MPCP

The simulated structure of MPCP was shown in Figure S21.

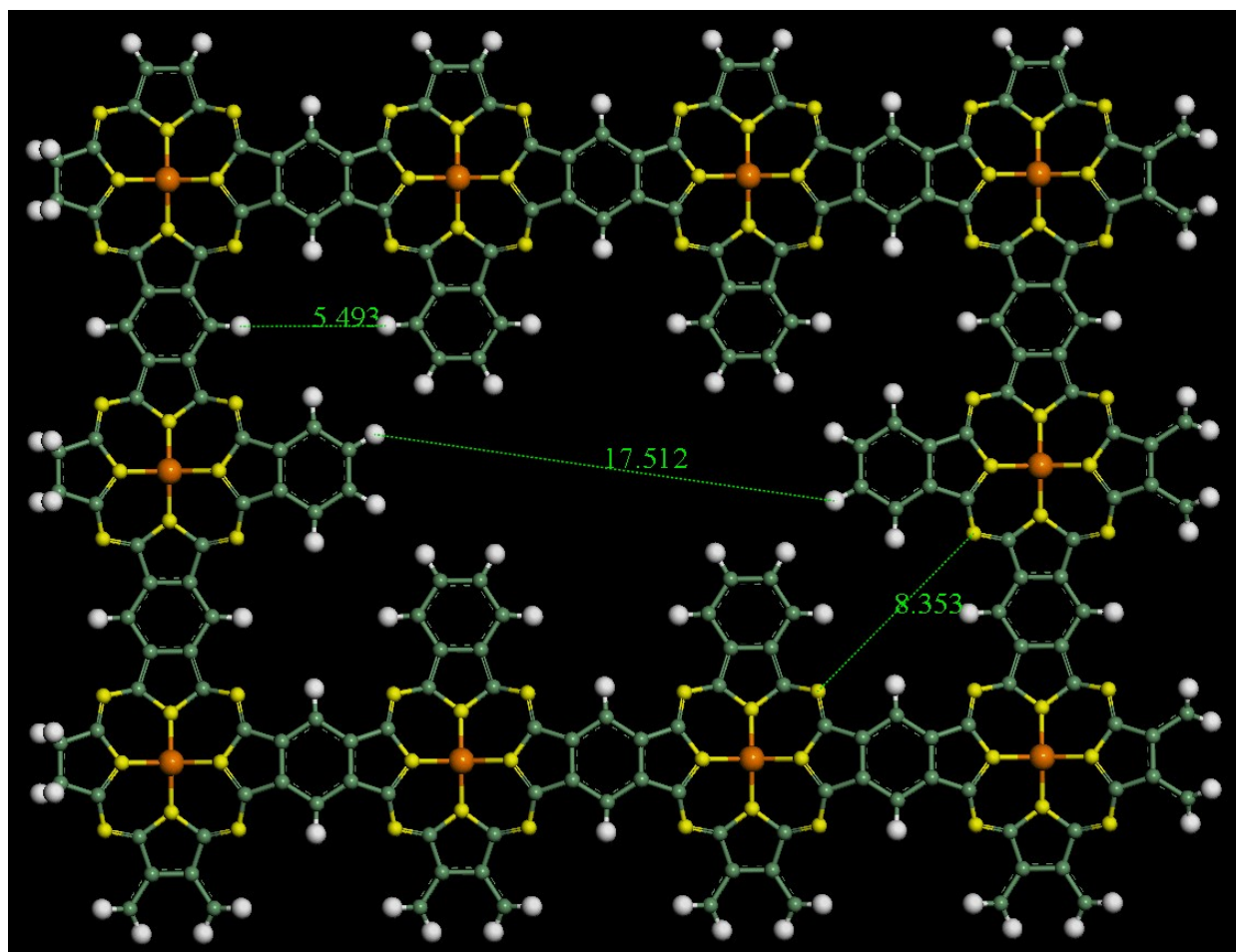


**Figure S21.** Simulated form of MPCP.

### Section 13. Simulated structure of PCP

The simulated structure of PCP was shown in Figure S22.

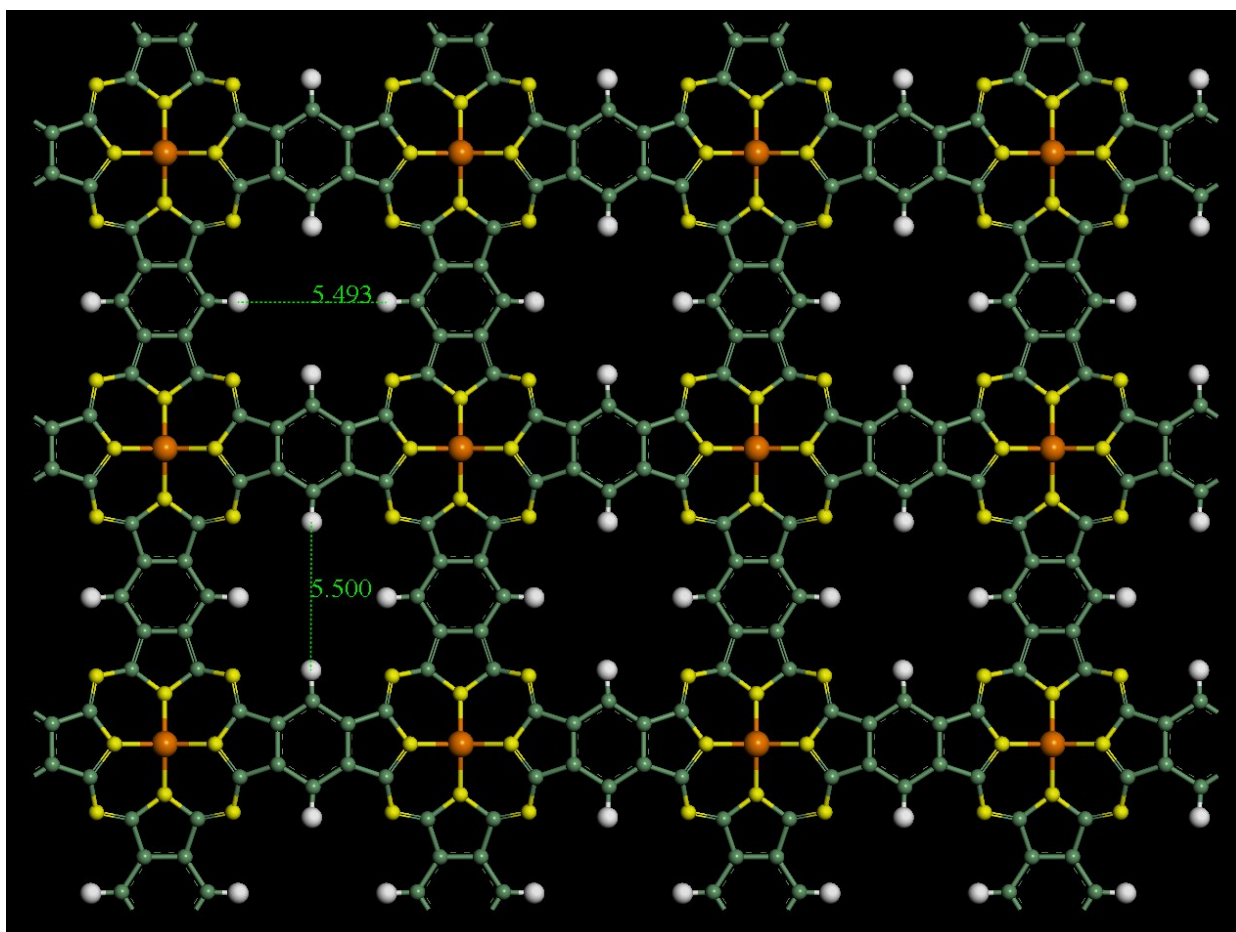


**Figure S22.** Simulated framework of PCP.

## Section 14. DFT calculation of reactants

Theoretical calculations of the reactants (DEM and TOX) were performed with Gaussian16<sup>[5]</sup> at the B3LYP-GD3(BJ)/def2SV(P) level of theory<sup>[6-8]</sup>. The optimized geometries were shown in Figure S23.

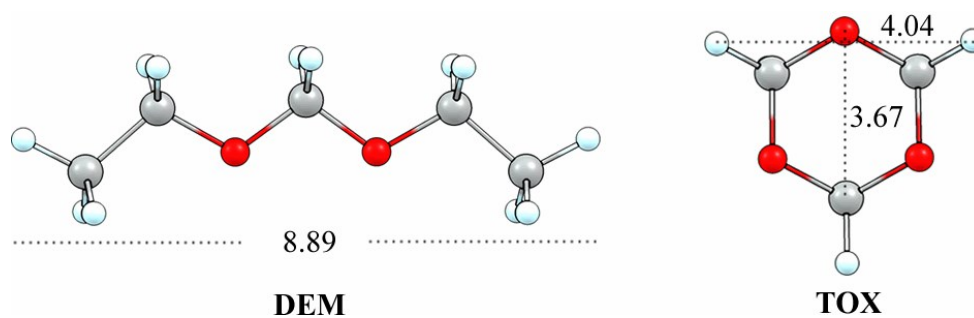


**Figure S23.** The optimized geometries of DEM and TOX. The atom distance is in angstrom.

## Coordinates

### DEM

|   |             |             |             |
|---|-------------|-------------|-------------|
| C | 3.47051700  | -0.56362700 | 0.00015100  |
| H | 4.44747000  | -0.04923300 | -0.00019500 |
| H | 3.41080600  | -1.20931500 | -0.89300000 |
| H | 3.41092600  | -1.20836000 | 0.89399900  |
| C | 2.33680500  | 0.44553000  | -0.00032300 |
| H | 2.40506800  | 1.10530800  | -0.89388300 |
| H | 2.40510800  | 1.10616500  | 0.89260000  |
| O | 1.11299500  | -0.25021300 | 0.00002500  |
| C | 0.00000000  | 0.57513600  | 0.00016800  |
| H | 0.00003400  | 1.24051600  | -0.90257800 |
| H | -0.00003400 | 1.24010500  | 0.90321700  |
| O | -1.11299500 | -0.25021200 | -0.00005600 |
| C | -2.33680500 | 0.44553000  | 0.00013300  |
| H | -2.40509300 | 1.10596800  | -0.89293700 |
| H | -2.40508300 | 1.10550500  | 0.89354500  |
| C | -3.47051700 | -0.56362700 | -0.00012200 |
| H | -3.41086200 | -1.20906800 | 0.89321200  |
| H | -4.44747000 | -0.04923300 | 0.00001500  |
| H | -3.41087100 | -1.20860800 | -0.89378800 |

### TOX

|   |             |             |             |
|---|-------------|-------------|-------------|
| C | -0.77337600 | -1.08158100 | 0.17364300  |
| C | 1.32344400  | -0.12887300 | 0.17352800  |
| C | -0.55007400 | 1.21046900  | 0.17374400  |
| H | -0.81294700 | -1.13667700 | 1.28811700  |
| H | -1.35800900 | -1.89930500 | -0.27008100 |
| H | 1.39130500  | -0.13543300 | 1.28798600  |
| H | 2.32380900  | -0.22629300 | -0.27047700 |
| H | -0.57809400 | 1.27193100  | 1.28823300  |
| H | -0.96597300 | 2.12572000  | -0.26976300 |
| O | -1.33341600 | 0.12990700  | -0.25763300 |
| O | 0.77915900  | 1.08991000  | -0.25747100 |
| O | 0.55425000  | -1.21982100 | -0.25733400 |

## References

- [1] H. Wu, Y. Cao, G. Zhu, D. Zeng, X. Zhu, J. Du, L. He, Chem. Commun. 2020, 56, 3637-3640.
- [2] H. H. Wu, M. Zeng, X. Zhu, C. C. Tian, B. B. Mei, Y. Song, X. L. Du, Z. Jiang, L. He, C. G. Xia, S. Dai, Chemelectrochem 2018, 5, 2717-2721.
- [3] G. Zhu, F. Zhao, D. Wang, C. Xia, J. Chromatogr. A 2017, 1513, 194-200.
- [4] D. Wang, F. Zhao, G. Zhu, C. Xia, Chem. Eng. J. 2018, 334, 2616-2624.
- [5] M. J. Frisch, G. W. Trucks, H. B. Schlegel, G. E. Scuseria, M. A. Robb, J. R. Cheeseman, G. Scalmani, V. Barone, G. A. Petersson, H. Nakatsuji, X. Li, M. Caricato, A. V. Marenich, J. Bloino, B. G. Janesko, R. Gomperts, B. Mennucci, H. P. Hratchian, J. V. Ortiz, A. F. Izmaylov, J. L. Sonnenberg, D. Williams-Young, F. Ding, F. Lipparini, F. Egidi, J. Goings, B. Peng, A. Petrone, T. Henderson, D. Ranasinghe, V. G. Zakrzewski, J. Gao, N. Rega, G. Zheng, W. Liang, M. Hada, M. Ehara, K. Toyota, R. Fukuda, J. Hasegawa, M. Ishida, T. Nakajima, Y. Honda, O. Kitao, H. Nakai, T. Vreven, K. Throssell, J. A. Montgomery, Jr., J. E. Peralta, F. Ogliaro, M. J. Bearpark, J. J. Heyd, E. N. Brothers, K. N. Kudin, V. N. Staroverov, T. A. Keith, R. Kobayashi, J. Normand, K. Raghavachari, A. P. Rendell, J. C. Burant, S. S. Iyengar, J. Tomasi, M. Cossi, J. M. Millam, M. Klene, C. Adamo, R. Cammi, J. W. Ochterski, R. L. Martin, K. Morokuma, O. Farkas, J. B. Foresman, and D. J. Fox, *Gaussian 16, Revision A.03*, Gaussian, Inc., Wallingford CT, 2016.
- [6] a) Becke, A. D. J. Chem. Phys. 1992, 96, 2155-2160; b) Becke, A. D. J. Chem. Phys. 1993, 98, 5648-5652; c) Lee, C.; Yang, W.; Parr, R. G. Phys. Rev. B 1988, 37, 785-789.
- [7] S. Grimme, S. Ehrlich and L. Goerigk, J. Comp. Chem. 2011, 32, 1456-1465.
- [8] a) F. Weigend and R. Ahlrichs, Phys. Chem. Chem. Phys., 2005, 7, 3297-305; b) F. Weigend, "Accurate Coulomb-fitting basis sets for H to Rn," Phys. Chem. Chem. Phys., 2006, 8, 1057-1065.